Cytokine 138 (2021) 155388

Contents lists available at ScienceDirect

Cytokine

journal homepage: www.elsevier.com/locate/cytokine

Tupaia guanylate-binding protein 1 interacts with vesicular stomatitis virus phosphoprotein and represses primary transcription of the viral genome

Tianle Gu [a,b], Dandan Yu [a,c,d], Ling Xu [a,c,d], Yu-Lin Yao [a,b], Xiao Zheng [a,e], Yong-Gang Yao [a,b,c,d,*]

[a] Key Laboratory of Animal Models and Human Disease Mechanisms of the Chinese Academy of Sciences & Yunnan Province, KIZ-CUHK Joint Laboratory of Bioresources and Molecular Research in Common Diseases, Kunming Institute of Zoology, Kunming, Yunnan 650223, China
[b] Kunming College of Life Science, University of Chinese Academy of Sciences, Kunming, Yunnan 650204, China
[c] Center for Excellence in Animal Evolution and Genetics, Chinese Academy of Sciences, Kunming, Yunnan 650223, China
[d] National Resource Center for Non-Human Primates, National Research Facility for Phenotypic & Genetic Analysis of Model Animals (Primate Facility), Kunming Institute of Zoology, Chinese Academy of Sciences, Kunming, Yunnan 650107, China
[e] School of Life Sciences, University of Science and Technology of China, Hefei, Anhui 230026, China

ARTICLE INFO

Keywords:
Tree shrew
guanylate-binding protein1 (GBP1)
Vesicular stomatitis virus (VSV)
Phosphoprotein
Nucleocapsid

ABSTRACT

Chinese tree shrews (*Tupaia belangeri chinensis*) are increasingly used as an alternative experimental animal to non-human primates in studying viral infections. Guanylate-binding proteins (GBP) belong to interferon (IFN)-inducible GTPases and defend the mammalian cell interior against diverse invasive pathogens. Previously, we identified five tree shrew *GBP* genes (*tGBP1*, *tGBP2*, *tGBP4*, *tGBP5*, and *tGBP7*) and found that tGBP1 showed antiviral activity against vesicular stomatitis virus (VSV) and type 1 herpes simplex virus (HSV-1) infections. Here, we showed that the anti-VSV activity of tGBP1 was independent of its GTPase activity and isoprenylation. In response to VSV infection, instead of regulating IFN expression and autophagy, tGBP1 competed with the VSV nucleocapsid (N) protein in binding to the VSV phosphoprotein (VSV-P), leading to the repression of the primary transcription of the VSV genome. These observations constitute the first report of the potential mechanism underlying the inhibition of VSV by GBP1.

1. Introduction

The innate immune response provides a robust first line of defense against viral infections [1] and relies on pattern recognition receptors (PRRs) to detect viral invasion and induce the expression of interferon (IFN) [2]. IFN subsequently induces the expression of hundreds of IFN-stimulated genes (ISGs), leading to a remarkable antiviral state [2–4]. The guanylate-binding protein 1 (GBP1) belongs to the GBP family, and can be induced by IFNs and inflammatory cytokines, such as tumor necrosis factor alpha (TNF-α) and interleukin-1β (IL-1β) [5–8]. GBP1 contains an N terminal GTPase domain and a C terminal domain (CTD) [5,9,10]. The GTPase domain endows GBP1 GTPase activity, which hydrolyzes guanosine-5′-triphosphate (GTP) to produce guanosine-5′-diphosphate (GDP) and guanosine-5′-monophosphate (GMP), whereas the CaaX motif in the CTD mediates protein isoprenylation of GBP1 [9,11–13].

With the coordination of other GBP family members, GBP1 protects the host from bacterial and parasitic infections by regulating vesicular traffic and protein complex assembly to stimulate oxidative, autophagic, membranolytic, and inflammasome-related antimicrobial activities within the cytosol, as well as in pathogen-containing vacuoles [10,13,14]. GBP1 is also involved in host innate immunity against viral infections [15]. Overexpression of GBP1 can control the replication of VSV [16], encephalomyocarditis virus (EMCV) [16], hepatitis C virus (HCV) [17], Kaposi's sarcoma-associated herpesvirus (KSHV) [18], and classical swine fever virus (CSFV) [19] in cell lines. The mechanism underlying the antiviral activity of GBP1 may vary dependent on the virus. GTPase activity is essential for GBP1-mediated antiviral effects against HCV [17] and CSFV [19]. Mutation of mouse *GBP2* (*mGBP2*, human *GBP1* ortholog in mice), which abrogates GTP binding activity, shows that the mutant mGBP2 still exhibits antiviral activity against VSV infection [20]. However, the different requirements of GTPase

* Corresponding author at: Key Laboratory of Animal Models and Human Disease Mechanisms of the Chinese Academy of Sciences & Yunnan Province, KIZ-CUHK Joint Laboratory of Bioresources and Molecular Research in Common Diseases, Kunming Institute of Zoology, Kunming, Yunnan 650223, China.
E-mail address: yaoyg@mail.kiz.ac.cn (Y.-G. Yao).

https://doi.org/10.1016/j.cyto.2020.155388
Received 23 August 2020; Received in revised form 22 November 2020; Accepted 23 November 2020
Available online 30 November 2020
1043-4666/

activity for GBP1 antiviral effects have not yet been fully elucidated. Understanding the mechanism of GBP1 antiviral function against different viruses will help define the role of GBP family members in innate immunity and in potential antiviral drug screening.

The Chinese tree shrew (*Tupaia belangeri chinensis*) is a squirrel-like, rat-sized mammal inhabiting the tropical forests of Southeast Asia and southern China [21,22]. It has many advantages as an experimental animal, including a close relationship to primates [23,24], small body size, low-cost maintenance, short reproductive cycle, and short life span [21,25–27]. In addition, tree shrews are susceptible to a wide range of human pathogenic viruses [26], including HCV [28], hepatitis B virus (HBV) [29], herpes simplex virus (HSV) [31], coxsackie virus [32], and SARS-CoV-2 [33]. Much effort has been expended to characterize the innate immune system of tree shrews to aid in their usage in the study of infectious diseases. In our previous studies, we characterized RIG-I like (RLR) receptors [34], Toll-like (TLR) receptors [35], MAVS [36,37], STING [38], 2′,5′-oligoadenylate synthetase family [39,40], and GBP family [41] in Chinese tree shrews, which has helped broaden our knowledge regarding innate immune genes in this species.

According to our previous study [41], there are five *GBP* genes (*tGBP1*, *tGBP2*, *tGBP4*, *tGBP5*, and *tGBP7*) in the Chinese tree shrew genome, and tGBP1 can control replication of VSV and HSV-1 in tree shrew renal cells [41]. In this study, we aimed to elucidate the underlying mechanism of tGBP1 antiviral activity against VSV. We found that the anti-VSV activity of tGBP1 was independent of its GTPase activity and isoprenylation. Mechanically, tGBP1 competed with the nucleocapsid protein to bind to the phosphoprotein of VSV, leading to the suppression of the primary transcription of the VSV genome.

2. Materials and methods

2.1. Experimental animals and cells

Chinese tree shrews were purchased from the Experimental Animal Core Facility of the Kunming Institute of Zoology (KIZ), Chinese Academy of Sciences (CAS). This study was approved by the Institutional Animal Care and Use Committee of KIZ, CAS.

Tree shrew primary renal cells (TSPRCs) were isolated, as described in our earlier studies [34,42]. Briefly, tree shrews were lethally anesthetized by a dose of pentobarbital. The kidneys were removed and minced into small pieces, then digested with 1 mg/mL DNase (Sigma, AMPD1-1KT) and 5 mg/mL collagenase type IV (Invitrogen, 17104019) solution for 45 min in a 37 °C water bath. After thrice washing with cold phosphate-buffered saline (PBS; Biological Industries, 0021517), the TSPRCs were resuspended and cultured at a density of 2×10^5 cells/mL in high-glucose Dulbecco's modified Eagles medium (DMEM; Gibco-BRL, 11965–092) supplemented with 10% fetal bovine serum (FBS; Gibco-BRL, 10099–141) and 1 × penicillin/streptomycin (Gibco-BRL, 10378016) at 37 °C in 5% CO_2 until confluence. The TSR6 (tree shrew renal cell #6) cell line was established in our previous study [43] and the HEK293T cell line was introduced from the Kunming Cell Bank, KIZ, CAS. These cells were cultured under the same conditions as the TSPRCs.

2.2. Reagents, antibodies, and plasmids

3-Methyladenine (3-MA; Sigma, M9281; autophagy inhibitor), cycloheximide (CHX; Sigma, 239763; protein biosynthesis inhibitor), and restriction enzymes *Bam*HI, *Xho*I, and T4 DNA ligase (Thermo Fisher Scientific) were utilized in this study. We also used the following antibodies: mouse monoclonal anti-Flag (Abmart, M20008), mouse monoclonal anti-β-actin (EnoGene, E1C602-2), mouse monoclonal anti-Myc (Invitrogen, MA1-21316-1MG), rabbit monoclonal anti-SQSTM1/P62 (Cell Signaling Technology; CST, 8025 T), rabbit monoclonal anti-LC3B (CST, 3868S), rabbit monoclonal anti-TBK1 (CST, 3504), and rabbit monoclonal anti-phospho-TBK1 (p-TBK1; Ser172) (CST, 5483).

The expression vectors for *Tupaia* MAVS (pCMV-tMAVS-3Tag-8, tMAVS) [36] and tGBP1 (pCMV-tGBP1-3Tag-8, tGBP1-WT) [41] were constructed in our previous studies [36,41]. We created two tGBP1 mutants (tGBP1-K51A and tGBP1-ΔCaaX) predicted to lose GTPase activity and protein isoprenylation, respectively. The tGBP1-ΔCaaX (pCMV-tGBP1-ΔCaaX-3Tag-8) mutant was subcloned from the tGBP1-WT (pCMV-tGBP1-3Tag-8) expression vector with *Bam*HI and *Xho*I. The tGBP1-K51A (pCMV-tGBP1-K51A-3Tag8) mutant was generated using multi-site-directed mutagenesis (Stratagene; 200518).

For the VSV-N and VSV-P constructs encoding the nucleocapsid (N) protein and phosphoprotein (P) of VSV, respectively, we first generated complementary DNA (cDNA) with total RNA extracted from the VSV-infected TSPRCs. The cDNA was used as the template to amplify the VSV-N and VSV-P coding regions using gene-specific primer pairs. The polymerase chain reaction (PCR) products were purified with the TIANquick Midi Purification Kit (Tiangen; DP204) and cloned into pCS2-N-Myc (pCS2-N-Myc-VSV-N and pCS2-N-Myc-VSV-P) or pCMV-3Tag-8 (pCMV-VSV-N-3Tag-8) using the ClonExpress® IIOne Step Cloning Kit (Vazyme; C112). The primers used in this study are listed in Table S1. All constructs were verified by sequencing.

2.3. RNA isolation and quantitative reverse transcription PCR (RT-qPCR)

Total RNA was extracted using an RNAsimple Total RNA Kit (Tiangen, DP419) according to the manufacturer's instructions. The cDNA was synthesized using M − MLV reverse transcriptase with a random primer (Promega, M1701). RT-qPCR was performed using iTaq Universal SYBRGreen Supermix (Bio-Rad, 1725124) supplemented with gene-specific primers (Table S1) on a CFX Connect Real-Time System (Bio-Rad, USA), as described in our prior research [34,35]. For data calculation, the indicated PCR product was serially diluted and 10^{-3}–10^{-10} dilution was used to generate standard curves. Ct values were measured with the respective standard curves. The tree shrew housekeeping gene *β-actin* was used as the reference gene for normalization.

2.4. Transfection, immunoprecipitation, and western blot analysis

Plasmids were transfected into cells using X-tremeGENE HP (Roche, 06366546001) following the manufacturer's instructions. Cells were lysed with RIPA lysis buffer (Beyotime, P0013) on ice and centrifuged at 12 000 × *g* at 4 °C for 10 min to remove cell debris. Protein concentration was determined using a BCA Protein Assay Kit (Beyotime, P0012). In total, 20 μg of protein was separated with 12% (vol/vol) sodium dodecyl sulphate (SDS)-polyacrylamide gel and electrophoretically transferred onto a polyvinylidene difluoride membrane (Bio-Rad, L1620177). Membranes were blocked with 5% (wt/vol) bovine serum albumin (BSA) in Tris-buffered saline (TBS) supplemented with 0.1% Tween-20 (TBST) (CST, #9997) at room temperature for 2 h, then incubated with respective primary antibodies against Myc (1:5 000), Flag (1:5 000), SQSTM1 (1:1 000), LC3B (1:1 000), p-TBK1 (1:1 000), TBK1 (1:1 000), and β-actin (1:10 000) overnight at 4 °C. After three washes with TBST (each 5 min), the membranes were incubated for 1 h with anti-mouse or anti-rabbit secondary antibodies (1:10 000, KPL, USA) at room temperature. The epitope was visualized using an ECL Western Blot Detection Kit (Millipore, WBKLS0500).

For immunoprecipitation, appropriate antibodies were incubated with protein G-agarose beads (15920010; Life Technologies) to form a complex for 2 h at room temperature. Cells were lysed with RIPA lysis buffer on ice for 1 h, followed by centrifugation at 12 000 × *g* for 10 min at 4 °C. Around 5% of the cell lysate was taken as input, while the remaining lysate was incubated with the antibody-protein G (Invitrogen, 10004D) bead complex at 4 °C overnight. After four washes with RIPA lysis buffer (each 5 min), the immunoprecipitates were separated by SDS-PAGE and analyzed by immunoblotting.

2.5. Virus infection

Vesicular stomatitis virus tagged by GFP (VSV-GFP) was initially obtained from Prof. Xinwen Chen, Wuhan Institute of Virology, CAS, Wuhan, China. This virus has a genomic integration of the *GFP* gene between the VSV-M and VSV-G genes, which facilitates the detection of viral replication. The virus was amplified as described in our previous studies [34,36]. For viral infection, cells seeded in 24-well (5×10^4/well) or 6-well plates (2×10^5/well) were washed three times with PBS (pH 7.4), incubated with VSV-GFP (multiplicity of infection (MOI) = 0.01) for 1 h in DMEM without FBS, and rinsed and cultured in fresh growth medium containing 1% FBS until harvest.

2.6. Virus adhesion, entry, genome transcription, and replication assays

For VSV replication, cells were seeded in 12-well (1×10^5/well) plates and infected with VSV-GFP (MOI = 0.01) for 12 h. The replication of VSV was quantified by flow cytometry, as described in our previous study [34].

The VSV adhesion, entry, and genome transcription assays were performed following a previous report [44] with some modification. In brief, TSPRCs were seeded in a 12-well plate (2×10^5/well) and infected with VSV-GFP (MOI = 1) for 1 h on ice to allow virus adhesion but impede entry. After three washes with PBS, the amount of cell-bound virus was measured by evaluating GFP mRNA via RT-qPCR. To analyze virus entry into cells via endocytosis, after virus adhesion for 1 h on ice, cells were washed three times with cold PBS, then incubated in pre-warmed growth medium for 5 min at 37 °C. After briefly washing with PBS, cells were treated with 0.25% trypsin for 10 min at 37 °C. Digestion was attenuated by adding 500 μL/well growth medium. The harvested cells were pelleted at 500 × g for 5 min at room temperature, then washed three times with PBS to remove any cell-associated virus that had not entered the cytoplasm. Total RNA was extracted from these cells to measure the number of viral genome copies that had entered cells by RT-qPCR assay. To assay virus genome transcription, after VSV-GFP (MOI = 1) adhesion for 1 h on ice, cells were washed three times with PBS and cultured in fresh growth medium (500 μL/well) supplied with CHX (100 μg/mL) to inhibit protein biosynthesis. Cells were harvested at different time points post-infection. Total RNA was extracted, and cDNA was synthesized using a combination of Oligo (dT) and *GFP* specific primer pairs (each primer 20 μg/mL) (Table S1). VSV genome transcription was measured as the *GFP* mRNA level.

2.7. Knockout of tupaia IFN alpha and beta receptor subunit 1 (tIFNAR1)

CRISPR/Cas9-mediated knockout of the *tIFNAR1* gene in TSR6 cells was performed according to our previously published procedure [43]. Briefly, sgRNA (Table S1) targeting the coding sequence of *tIFNAR1* was designed and cloned into the pX330-T7 vector (a kind gift from Dr. Ping Zheng, KIZ) expressing mCherry. TSR6 cells were transfected with the pX330-T7 plasmid carrying sgRNA. Single cells were manually picked from the successfully transfected cells and cultured for three weeks for expansion. The genomic DNA of the expanded single cells was extracted using an AxyPrep Multisource Genomic DNA Miniprep Kit (Axygen, 26817KC1). The gene region spanning the sgRNA targeting site was amplified using a specific primer pair (Table S1) and cloned into T-Vector pMD19 (Takara, 6013) for transformation. About 10 clones were randomly picked for sequencing validation. We also attempted to verify knockout of the tIFNAR1 protein using the IFNAR1 monoclonal antibody (Santa Cruz, sc-7391), which targets human IFNAR1 (hIFNAR1). However, we failed to detect tIFNAR1 using this antibody, possibly because of the low sequence conservation between tIFNAR1 and hIFNAR1 proteins.

2.8. Statistical analysis

Statistical analysis was performed using unpaired Student's *t* test (two-tailed) with GraphPad Prism software. Significant values were indicated at * $P < 0.05$ and ** $P < 0.01$. Results are represented as means ± standard deviation (SD).

3. Results

3.1. GTPase activity and protein isoprenylation of tGBP1 were independent of anti-VSV activity

In humans and mice, GBP1 contains a GTPase domain and a CaaX motif, which mediate GBP1 GTPase activity and protein isoprenylation, respectively [9,11–13]. Sequence alignment analysis revealed that tGBP1 also has a GTPase domain and CaaX motif, and thus we deduced that tGBP1 may have GTPase activity and may be isoprenylated. GTPase activity and isoprenylation are very important for maintaining GBP1 function [7,45]. GTPase activity is required for GBP1 to inhibit HCV in humans [17] and CSFV in pigs [19], whereas GTP binding activity is not essential for mGbp2 to control VSV infection [20]. We earlier demonstrated that tGBP1 can inhibit VSV infection in tree shrew renal cells [41]. Thus, we checked whether GTPase activity and protein isoprenylation are essential for tGBP1 inhibition of VSV infection. We generated the tGBP1-K51A and tGBP1-ΔCaaX mutants predicted to abrogate GTPase activity and protein isoprenylation of tGBP1, respectively, as described in previous study [18] (Fig. 1A). Overexpression of tGBP1-WT and the two mutants (tGBP1-K51A and tGBP1-ΔCaaX) equally inhibited VSV replication in TSPRCs (Fig. 1B–D and Figure S1).

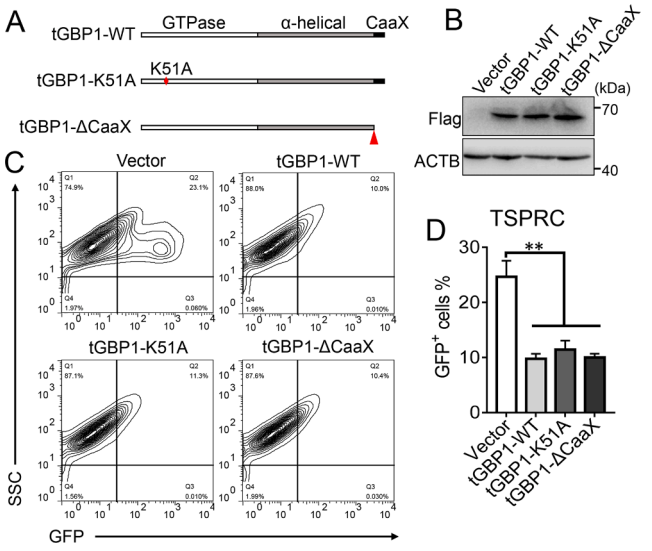

Fig. 1. GTPase activity and protein isoprenylation of tGBP1 were dispensable for its antiviral function against VSV. (A) Schematic of wild-type tGBP1 (tGBP1-WT, pCMV-tGBP1-3Tag-8) and two mutants (tGBP1-K51A, pCMV-tGBP1-K51A-3Tag-8; tGBP1-ΔCaaX, pCMV-tGBP1-ΔCaaX-3Tag-8). (B) Successful overexpression of wild-type tGBP1 and its mutants in TSPRCs. Cells (2×10^5) were transiently transfected with indicated expression vectors for tGBP1-WT, tGBP1-K51A, tGBP1-ΔCaaX and empty vector (Vector), respectively. (C,D) Flow cytometry analysis for VSV replication in TSPRCs with overexpression of tGBP1 and its mutants. Cells (1×10^5) were transiently transfected with empty vector (Vector), tGBP1-WT, tGBP1-K51A, and tGBP1-ΔCaaX for 12 h, then infected by VSV-GFP (0.01 MOI). Replication of VSV in TSPRCs overexpressing indicated vectors was quantified by expression level of GFP at 12 h post-infection (C). Percentage of 10 000 cells expressing GFP (GFP^+ cells) was counted and values are presented as means ± SD (D). Experiments were independently repeated three times with similar results, and each experiment had two biological repeats. Results shown are a representative experiment. Values are means ± SD (n = 2 biological repeats). ** $P < 0.01$ two-tailed unpaired Student's *t*-test.

These results revealed that GTPase and isoprenylation may be dispensable for tGBP1 to inhibit VSV replication.

3.2. tGBP1 restricted VSV, but not by regulating IFN expression or autophagy

In humans, hGBP4 is involved in regulation of IFN expression upon Sendai virus infection [46], while hGBP1 affects autophagy in response to *Chlamydia trachomatis* infection [47]. We tested whether tGBP1 plays a similar role as hGBP1 in affecting autophagy or as hGBP4 in regulating IFN expression. Overexpression of tGBP1 in TSPRCs did not up-regulate *tIFNB1* mRNA expression (Fig. 2A) and had a repressive effect on *tIFNB1* expression relative to the control group at 9 h post VSV infection (Fig. 2A). Consistent with our previous study [36], overexpression of tMAVS (a positive control) resulted in a significant induction of *tIFNB1* expression. In accordance with this result, phosphorylation of TBK1 was up-regulated in response to VSV, with a peak at 6 h post VSV infection. Overexpression of tGBP1 postponed the phosphorylation of TBK1, with a delayed peak at 12 h (Fig. 2B and Figure S2).

When autophagy is activated in cells, there is an increase in the phosphatidylethanolamine-conjugated form of the LC3B(LC3-II)/LC3B-I ratio and a decrease in SQSTM1 [48]. We found that the levels of SQSTM1 and LC3B-II/LC3B-I were not significantly altered in the cells upon VSV-GFP infection, and tGBP1 overexpression also had no apparent effect on autophagy activation (Fig. 2B and Figure S2). These results indicate that IFN signaling and autophagy may not be actively involved in tGBP1 inhibition of VSV.

To further validate the role of IFN signaling and autophagy in tGBP1 inhibition of VSV replication, we generated TSR6 cells with *tIFNAR1* knockout (tIFNAR1-KO cells; Figure S3). Deficiency of IFNAR1 can abrogate the antiviral function of type I IFN [4,49,50]. We checked the antiviral activity of tGBP1 in tIFNAR1-KO TSR6 cells. The replication of VSV increased in the tIFNAR1-deficient TSR6 cells compared to wild-type TSR6 cells, consistent with previous study showing that type I IFN can significantly restrict VSV infection [1] (Fig. 3A and B). Deficiency of IFNAR1 did not alter the antiviral pattern of tGBP1 against VSV, although the inhibition effect of tGBP1 on VSV decreased slightly (Fig. 3A and B), suggesting that type I IFN may have a minor role in the anti-VSV activity of tGBP1. Pharmacological inhibition of autophagy by 3-MA in TSPRCs enhanced VSV-GFP replication relative to the untreated group (Fig. 3C and D). Inhibition of autophagy did not affect the anti-VSV effect of tGBP1 (Fig. 3C and D). Taken together, these results demonstrate that the antiviral effects of tGBP1 on VSV infection may not be mediated by the altered expression of IFN or autophagy.

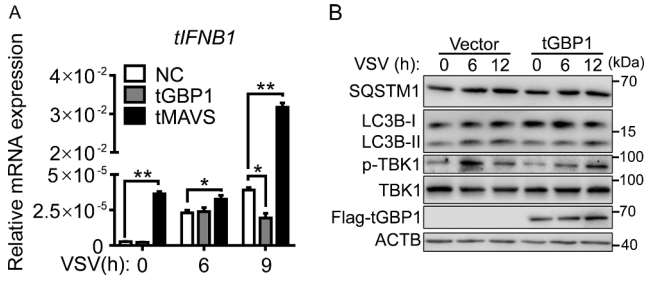

Fig. 2. tGBP1 did not affect autophagy but showed delayed inhibition of *tIFNB1* mRNA expression in response to VSV infection. (A) mRNA levels of *tIFNB1* in TSPRCs with or without overexpression of tGBP1 upon VSV infection. TSPRCs (5×10^4) were transiently transfected with pCMV-3Tag-8 (empty vector, NC), pCMV-tGBP1-3Tag-8 (tGBP1), and pCMV-tMAVS-3Tag-8 (tMAVS, used as a positive control for up-regulating *tIFNB1* mRNA upon VSV infection) for 12 h, then infected with VSV-GFP (0.01 MOI) for indicated times. mRNA expression of *tIFNB1* was analyzed by RT-qPCR. (B) Protein levels of autophagy-related proteins, p-TBK1, and TBK1 in TSPRCs with or without overexpression of tGBP1 upon VSV infection. TSPRCs (2×10^5) were transiently transfected with pCMV-3Tag-8 (Vector) and pCMV-tGBP1-3Tag-8 (tGBP1) for 12 h and infected by VSV-GFP (0.01 MOI) for indicated times. Protein level of ACTB was used as a loading control for western blotting. Experiments were independently repeated three times with similar results. Results shown are from a representative experiment. Values are means ± SD (n = 3 biological repeats). * $P < 0.05$, ** $P < 0.01$, two-tailed unpaired Student's *t*-test.

3.3. tGBP1 repressed genomic transcription of VSV

As the above results showed that tGBP1 played no active role in regulation of host IFN expression or autophagy, but did have an antiviral effect on VSV replication, we speculated that tGBP1 may directly inhibit VSV infection by impairing specific processes in viral replication. VSV is a negative-strand RNA virus (family *Rhabdoviridae*) that establishes infection via adhesion to the host cell surface [51]. Once it enters the cell through endocytosis, the negative-strand genomic RNA is used as a template for transcription of viral mRNAs and for RNA replication [51]. To map the viral replication step(s) targeted by tGBP1, we measured the effect of tGBP1 on VSV adhesion, entry, and genomic transcription following a modified procedure from previous research [44] (Fig. 4A). Overexpression of tGBP1 in TSPRCs did not affect VSV adhesion and entry, as manifested by the similar levels of *GFP* mRNA between cells with or without tGBP1 overexpression (Fig. 4B). However, the transcription of the viral genome was significantly repressed by overexpression of tGBP1 as early as 30 min post VSV infection (Fig. 4C). These results indicate that tGBP1 exerted its antiviral effects against VSV by repressing viral genomic transcription.

3.4. tGBP1 bound to VSV phosphoprotein

Three VSV proteins, including nucleoprotein (VSV-N, which coats viral RNA), large protein (VSV-L, which possesses all viral enzymes necessary for transcription), and phosphoprotein (VSV-P, which binds to both VSV-N and VSV-L to stimulate RNA synthesis), are necessary for the genomic transcription of VSV [52,53]. We tested whether tGBP1 interacts with these viral proteins. Because we failed to make a correct plasmid for overexpressing the VSV-L protein, we focused on the potential interaction between tGBP1 and VSV-P and between tGBP1 and VSV-N. Co-immunoprecipitation experiments showed that tGBP1 interacted with VSV-P, but not with VSV-N (Fig. 5A). As VSV-P interacts with both VSV-N and VSV-L during VSV genomic transcription [52] and because tGBP1 selectively interacted with VSV-P but not VSV-N (Fig. 5A), tGBP1 may impair the interaction between VSV-P and VSV-N. In line with this speculation, we found that overexpression of tGBP1 reduced the interaction between VSV-P and VSV-N (Fig. 5B and Figure S4). These results demonstrate that tGBP1 can impair the interaction between VSV-P and VSV-N by specifically binding to VSV-P.

4. Discussion

Chinese tree shrews have received growing attention as small, viable experimental animals [21,26]. Their closer affinity to primates compared to rodents has opened a new avenue for replacing primates in biomedical research and creating animal models of human diseases [21–25,27,33,54,55]. We previously studied *tGBPs* and found that tGBP1 had an antiviral effect on VSV [41]. In this study, we found that tGBP1 inhibited VSV replication by repressing primary transcription of the VSV genome. tGBP1 interacted with VSV-P and impaired the interaction between VSV-N and VSV-P, which may account for the antiviral function of tGBP1 against VSV. This anti-VSV activity of tGBP1 was independent of its GTPase activity and isoprenylation, in line with previous research on mGbp2 [20].

GBP1 has a broad spectrum of antiviral activity for a variety of viruses, such as VSV [16], EMCV [16], HCV [17], CSFV [19], and KSHV [18]. Many ISGs inhibit viral replication by positively regulating type I IFN expression [4] and autophagy [56,57]. Research has shown that hGBP1/2 mediates the restriction of *Chlamydia trachomatis* growth via

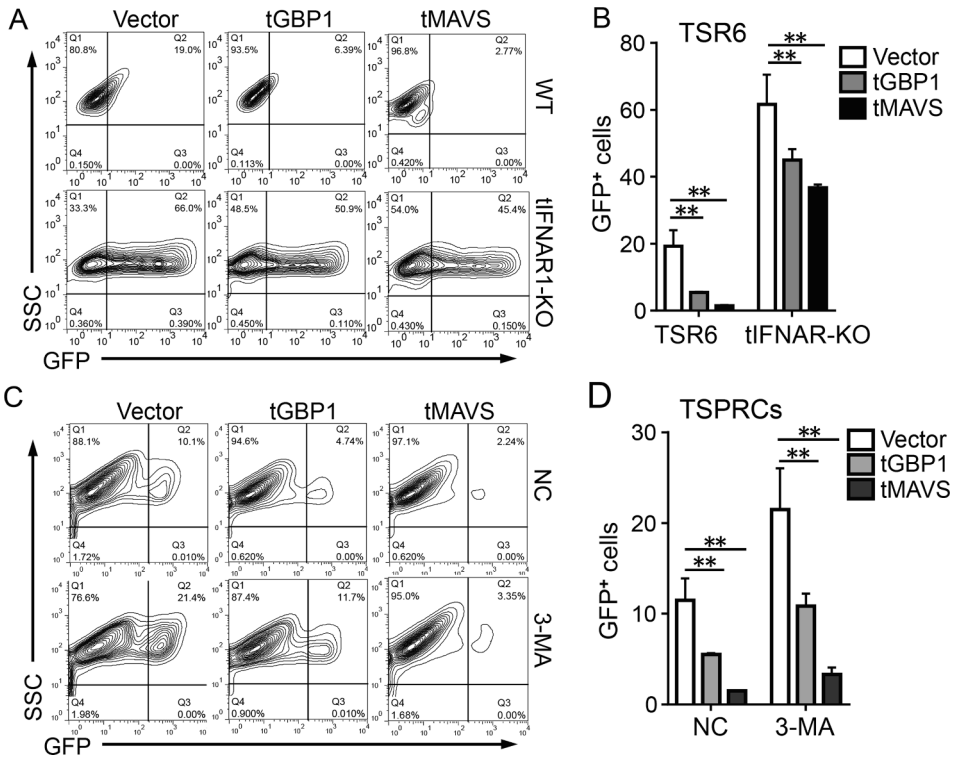

Fig. 3. Anti-VSV activity of tGBP1 was independent of IFN signaling and autophagy. (A-B) Flow cytometry analysis (A) and quantification (B) of VSV replication. TSR6 cells with knockout of IFNAR1 (tIFNAR1-KO) or wild-type cells (WT) were seeded in 12-well plates (1×10^5) and transiently transfected with pCMV-3Tag-8 (empty vector, Vector), pCMV-tGBP1-3Tag-8 (tGBP1), and pCMV-tMAVS-3Tag-8 (tMAVS, used as a positive control for inhibiting VSV replication) for 12 h, respectively, followed by VSV-GFP (0.01 MOI) infection for 12 h. Procedure for detecting VSV replication was the same as in Fig. 1C-D. (C-D) Autophagy inhibition had no effect on tGBP1 antiviral activity. TSPRCs (1×10^5 cells/well in 12-well plates) were transfected with pCMV-3Tag-8 (empty vector, Vector), pCMV-tGBP1-3Tag-8 (tGBP1), and pCMV-tMAVS-3Tag-8 for 12 h, respectively, followed by VSV-GFP (0.01 MOI) infection, with or without 3-methyladenine (3-MA, 5 μM) treatment for 12 h before harvest. All data in (A) and (C) are representative of three independent experiments with similar results. Bars in (B) and (D) represent means ± SD (n = 2 biological repeats). **, $P < 0.01$, two-tailed Student's *t*-test.

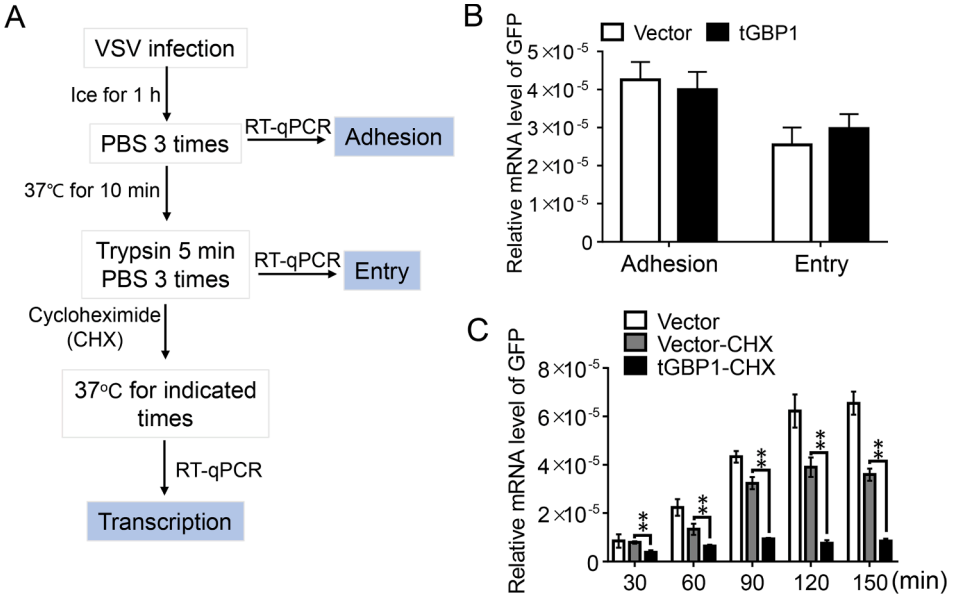

Fig. 4. tGBP1 impaired VSV genomic transcription. (A) Flow chart of viral adhesion, entry, and transcription assays. (B) TSPRCs were transfected with pCMV-3Tag-8 (empty vector, Vector) and pCMV-tGBP1-3Tag-8 (tGBP1) for 12 h, respectively, then infected with VSV-GFP (1 MOI) and incubated on ice for 1 h (for adhesion group), followed by further incubation at 37 °C for 5 min (for entry group). Relative level of *GFP* mRNA was determined by RT-qPCR. (C) TSPRCs were transiently transfected with empty vector and tGBP1 expression vector for 12 h. Cells were then infected by VSV-GFP (1 MOI), together with or without cycloheximide (CHX, 100 μg/mL), and harvested at indicated time points. Experiments were independently repeated three times with similar results. Results shown are a representative experiment. Values are means ± SD (n = 3 biological repeats). ** $P < 0.01$, two-tailed unpaired Student's *t*-test.

autophagy [47]. Here, however, overexpression of tGBP1 in TSPRCs neither up-regulated *tIFNB1* mRNA expression nor enhanced autophagy in response to VSV infection. In line with these observations, inhibition of autophagy by 3-MA had no effect on the anti-VSV activity of tGBP1. Deficiency of tIFNAR1 slightly decreased the inhibition effect of tGBP1 on VSV replication. This may be a consequence of increased replication of VSV upon tIFNAR1 knockout, or may explain why type I IFN plays a minor role in the anti-VSV function of tGBP1 by promoting the translocation or aggregation of tGBP1, which are important for its function but yet to be clarified in the case of VSV [58–61]. Thus, GBP1 may exert its anti-VSV function though impairing specific processes in viral replication, but not by regulating host immune reactions to counteract VSV infection. Consistent with this speculation, the primary transcription of the VSV genome was restrained by overexpression of tGBP1 in TSPRCs. This finding provides a novel mechanism regarding the antiviral role of GBP1.

VSV is a negative-strand RNA virus belonging to the family *Rhabdoviridae* [51]. Viral genome transcription is the first RNA biosynthetic step after cellular entry and uncoating to release its viral ribonucleocapsid template [51]. Transcription is carried out by an RNA-dependent RNA polymerase whose major components are the L protein catalytic subunit and P cofactor [51]. The active template for transcription is the RNA genome encapsidated with the VSV-N protein [51]. The VSV-P protein binds to L and template-associated N to form a N-RNA:P-L

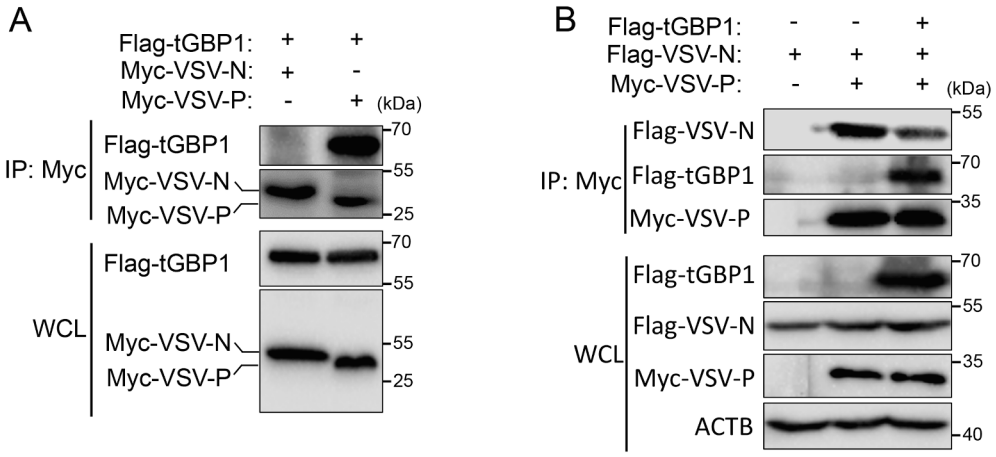

Fig. 5. tGBP1 bound to phosphoprotein and competed with nucleocapsid protein of VSV. (A) HEK293T cells (1×10^7) were co-transfected with a combination of pCMV-tGBP1-3Tag-8 (Flag-tGBP1) and pCS2-N-Myc-VSV-N (Myc-VSV-N) or a combination of pCMV-tGBP1-3Tag-8 (Flag-tGBP1) and pCS2-N-Myc-VSV-P (Myc-VSV-P) (5 μg each) for 24 h before harvest. (B) HEK293T cells (1×10^7) were co-transfected with a combination of pCS2-N-Myc-VSV-P (Myc-VSV-P) and pCMV-VSV-N-3Tag-8 (Flag-VSV-N), together with empty vector or pCMV-tGBP1-3Tag-8 (Flag-tGBP1) (5 μg each) for 24 h before harvest. Immunoprecipitation (IP) and western blotting assays were performed. WCL - whole cell lysates. Experiments in (A-B) were independently repeated two times with similar results. Results shown are a representative experiment.

complex, which is essential for transcription of viral mRNA *in vitro* [51–53]. Here, tGBP1 specifically interacted with VSV-P, but not VSV-N; this interaction impaired the association between VSV-P and VSV-N and may hinder N-RNA:P-L complex formation. Unfortunately, we could not answer the question whether the interaction between tGBP1 and VSV-P affects the binding of VSV-P to VSV-L because we did not have an expression vector for VSV-L. Our tGBP1 results are consistent with previous research showing that TRIM69 inhibits the transcription of the incoming virion-associated negative-strand RNA of VSV by interacting with the VSV-P protein [53]. Targeting the VSV-P protein and subsequently preventing the synthesis of viral mRNA may be a general strategy for host inhibition of VSV replication and for the design of potential antiviral drugs.

GTPase activity of GBP1 is essential for inhibiting human HCV [17] and pig CSFV infections [19]. In this study, we found that GTPase of tGBP1 was not essential for inhibiting VSV replication. This result indicates that GBP1 may adopt a different mechanism to exert antiviral functions in response to different viral infections. Both HCV and CSFV are positive-sense RNA viruses that replicate on membranous structures in the cytoplasm called replication complexes (RCs) [61–63]. RCs provide an advantageous microenvironment for viral replication [61,63]. It has been reported that mGBPs can target the positive-sense RNA virus murine norovirus (MNV) RCs via the LC3 conjugation system of autophagy upon their induction by IFN-γ [61]. A similar mechanism exists for the inhibition of *Toxoplasma gondii* infection by mGBPs via targeting the parasitophorous vacuole membrane (PVM) [60,64,65]. Therefore, GTPase is crucial for the recruitment of GBP to RCs [61] and PVM [7,10,66]. In contrast to HCV and CSFV, VSV is a negative-strand RNA virus that replicates in the cytoplasm of host cells, without potential protection by specific membrane complexes formed by the pathogen. Our results suggest that tGBP1 inhibited VSV replication by competing with the VSV-N protein in binding to VSV-P. This competitive interaction among tGBP1, VSV-P, and VSV-N was unrelated to the membrane targeting of GBP1, which is dependent on its GTPase activity. The different strategies of GBP1 to inhibit the replication of VSV versus the infection of HCV or CSFV suggests a multifaceted role of GBP1 as a cellular effector of innate immunity. It should be mentioned that the causal link of tGBP1 and VSV-P binding and inhibition of viral transcription were not shown in this study. Generation of tGBP1 mutants with the loss of VSV-P binding and testing whether these mutants are associated with loss of antiviral activity should help resolve this issue.

In summary, our findings showed that tGBP1 inhibited VSV replication by repressing primary transcription of its genomes via competing with VSV-N in binding to VSV-P (Fig. 6), without the potential involvement of IFN expression or autophagy. This provides new insight into the diverse mechanisms of the antiviral function of GBP1 in host innate immunity.

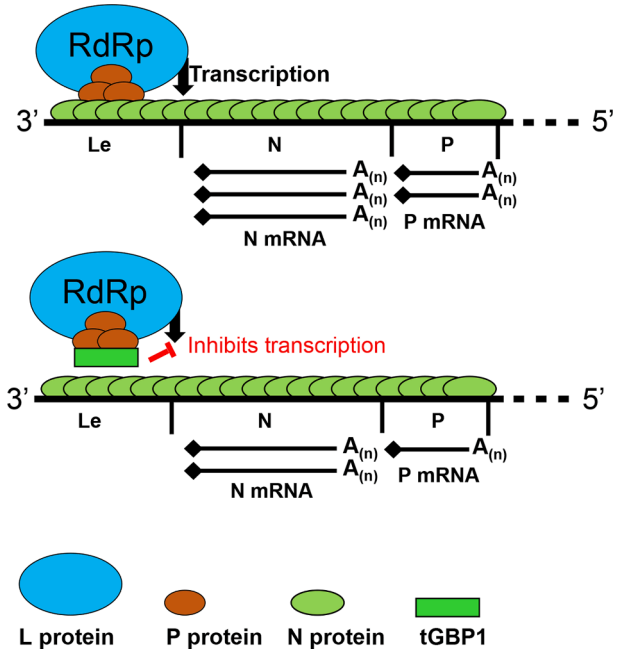

Fig. 6. Model for tGBP1 repression of VSV genome transcription. During VSV transcription, RdRp, a complex of L and trimer P, binds to N encapsidated RNA genome to form a transcription complex and initiate mRNA synthesis (upper panel). tGBP1 specifically binds to P but not N and impairs interaction between P and N, which may hinder formation of transcription complex and VSV genome transcription (lower panel). RdRp, RNA-dependent RNA polymerase; L protein, large protein; P protein, phosphoprotein; N protein, nucleoprotein.

CRediT authorship contribution statement

Tianle Gu: Investigation, Methodology, Writing - original draft. **Dandan Yu:** Funding acquisition, Data curation. **Ling Xu:** Methodology, Resources, Software. **Yu-Lin Yao:** Methodology, Resources, Software. **Xiao Zheng:** Methodology, Resources, Software. **Yong-Gang Yao:** Funding acquisition, Supervision, Writing - review & editing.

Declaration of Competing Interest

The authors declare that they have no known competing financial interests or personal relationships that could have appeared to influence the work reported in this paper.

Acknowledgments

This study was supported by the National Natural Science Foundation of China (U1902215 to Y-GY and 81571998 to YDD), Yunnan Province (202001AS070023 to YDD), and Chinese Academy of Sciences (Light of West China Program xbzg-zdsys-201909 to Y-GY). We would like to thank Guolan Ma and Cong Li for their technical support in flow cytometry.

Appendix A. Supplementary material

Supplementary data to this article can be found online at https://doi.org/10.1016/j.cyto.2020.155388.

References

[1] F. McNab, K. Mayer-Barber, A. Sher, A. Wack, A. O'Garra, Type I interferons in infectious disease, Nat. Rev. Immunol. 15 (2) (2015) 87–103.
[2] S. Akira, S. Uematsu, O. Takeuchi, Pathogen recognition and innate immunity, Cell 124 (4) (2006) 783–801.
[3] D. Goubau, S. Deddouche, E.S.C. Reis, Cytosolic sensing of viruses, Immunity 38 (5) (2013) 855–869.
[4] W.M. Schneider, M.D. Chevillotte, C.M. Rice, Interferon-stimulated genes: a complex web of host defenses, Annu. Rev. Immunol. 32 (2014) 513–545.
[5] M.A. Olszewski, J. Gray, D.J. Vestal, In silico genomic analysis of the human and murine guanylate-binding protein (GBP) gene clusters, J. Interferon Cytokine Res. 26 (5) (2006) 328–352.
[6] D. Degrandi, C. Konermann, C. Beuter-Gunia, A. Kresse, J. Wurthner, S. Kurig, S. Beer, K. Pfeffer, Extensive characterization of IFN-induced GTPases mGBP1 to mGBP10 involved in host defense, J. Immunol. 179 (11) (2007) 7729–7740.
[7] K. Tretina, E.-S. Park, A. Maminska, J.D. MacMicking, Interferon-induced guanylate-binding proteins: Guardians of host defense in health and disease, J. Exp. Med. 216 (3) (2019) 482–500.
[8] C. Lubeseder-Martellato, E. Guenzi, A. Jorg, K. Topolt, E. Naschberger, E. Kremmer, C. Zietz, E. Tschachler, P. Hutzler, M. Schwemmle, K. Matzen, T. Grimm, B. Ensoli, M. Sturzl, Guanylate-binding protein-1 expression is selectively induced by inflammatory cytokines and is an activation marker of endothelial cells during inflammatory diseases, Am. J. Pathol. 161 (2002).
[9] B. Prakash, G.J.K. Praefcke, L. Renault, A. Wittinghofer, C. Herrmann, Structure of human guanylate-binding protein 1 representing a unique class of GTP-binding proteins, Nature 403 (2000) 567.
[10] B.H. Kim, A.R. Shenoy, P. Kumar, C.J. Bradfield, J.D. MacMicking, IFN-inducible GTPases in host cell defense, Cell Host Microbe 12 (4) (2012) 432–444.
[11] M. Schwemmle, P. Staeheli, The interferon-induced 67-kDa guanylate-binding protein (hGBP1) is a GTPase that converts GTP to GMP, J. Biol. Chem. 269 (1994).
[12] A. Ghosh, G.J. Praefcke, L. Renault, A. Wittinghofer, C. Herrmann, How guanylate-binding proteins achieve assembly-stimulated processive cleavage of GTP to GMP, Nature 440 (7080) (2006) 101–104.
[13] E. Meunier, P. Broz, Interferon-inducible GTPases in cell autonomous and innate immunity, Cell. Microbiol. 18 (2) (2016) 168–180.
[14] B.H. Kim, A.R. Shenoy, P. Kumar, R. Das, S. Tiwari, J.D. MacMicking, A family of IFN-gamma-inducible 65-kD GTPases protects against bacterial infection, Science 332 (6030) (2011) 717–721.
[15] D. Pilla-Moffett, M.F. Barber, G.A. Taylor, J. Coers, Interferon-inducible GTPases in host resistance, inflammation and disease, J. Mol. Biol. 428 (17) (2016) 3495–3513.
[16] S.L. Anderson, J.M. Carton, J. Lou, L. Xing, B.Y. Rubin, Interferon-induced guanylate binding protein-1 (GBP-1) mediates an antiviral effect against vesicular stomatitis virus and encephalomyocarditis virus, Virology 256 (1) (1999) 8–14.
[17] Y. Itsui, N. Sakamoto, S. Kakinuma, M. Nakagawa, Y. Sekine-Osajima, M. Tasaka-Fujita, Y. Nishimura-Sakurai, G. Suda, Y. Karakama, K. Mishima, M. Yamamoto, T. Watanabe, M. Ueyama, Y. Funaoka, S. Azuma, M. Watanabe, Antiviral effects of the interferon-induced protein guanylate binding protein 1 and its interaction with the hepatitis C virus NS5B protein, Hepatology 50 (6) (2009) 1727–1737.
[18] Z. Zou, Z. Meng, C. Ma, D. Liang, R. Sun, K. Lan, Guanylate-binding protein 1 inhibits nuclear delivery of Kaposi's sarcoma-associated herpesvirus virions by disrupting formation of actin filament, J. Virol. 91 (16) (2017) e00632–e717.
[19] L.F. Li, J. Yu, Y. Li, J. Wang, S. Li, L. Zhang, S.L. Xia, Q. Yang, X. Wang, S. Yu, Y. Luo, Y. Sun, Y. Zhu, M. Munir, H.J. Qiu, Guanylate-binding protein 1, an interferon-induced GTPase, exerts an antiviral activity against classical swine fever virus depending on its GTPase activity, J. Virol. 90 (9) (2016) 4412–4426.
[20] C.C. Carter, V.Y. Gorbacheva, D.J. Vestal, Inhibition of VSV and EMCV replication by the interferon-induced GTPase, mGBP-2: differential requirement for wild-type GTP binding domain, Arch. Virol. 150 (6) (2005) 1213–1220.
[21] Y.G. Yao, Creating animal models, why not use the Chinese tree shrew (*Tupaia belangeri chinensis*)? Zool. Res. 38 (3) (2017) 118–126.
[22] Y. Peng, Z., Z. Ye, Z., R. Zou, J., Y. Wang, X., B. Tian, P., Y. Ma, Y., L. Shi, M., Biology of Chinese tree shrews, Kunming: Yunnan Science and Technology Press (in Chinese) (1991).
[23] Y. Fan, Z.Y. Huang, C.C. Cao, C.S. Chen, Y.X. Chen, D.D. Fan, J. He, H.L. Hou, L. Hu, X.T. Hu, X.T. Jiang, R. Lai, Y.S. Lang, B. Liang, S.G. Liao, D. Mu, Y.Y. Ma, Y. Y. Niu, X.Q. Sun, J.Q. Xia, J. Xiao, Z.Q. Xiong, L. Xu, L. Yang, Y. Zhang, W. Zhao, X. D. Zhao, Y.T. Zheng, J.M. Zhou, Y.B. Zhu, G.J. Zhang, J. Wang, Y.G. Yao, Genome of the Chinese tree shrew, Nat. Commun. 4 (2013) 1426.
[24] Y. Fan, M.S. Ye, J.Y. Zhang, L. Xu, D.D. Yu, T.L. Gu, Y.L. Yao, J.Q. Chen, L.B. Lv, P. Zheng, D.D. Wu, G.J. Zhang, Y.G. Yao, Chromosomal level assembly and population sequencing of the Chinese tree shrew genome, Zool. Res. 40 (6) (2019) 506–521.
[25] J. Xiao, R. Liu, C.S. Chen, Tree shrew (*Tupaia belangeri*) as a novel laboratory disease animal model, Zool. Res. 38 (3) (2017) 127–137.
[26] R. Li, M. Zanin, X. Xia, Z. Yang, The tree shrew as a model for infectious diseases research, J. Thorac. Dis. 10 (Suppl 19) (2018) S2272–S2279.
[27] Y.T. Zheng, Y.G. Yao, L. Xu, Basic biology and disease models of tree shrews, Kunming: Yunnan Science and Technology Press, (in Chinese), 2014.
[28] Y. Amako, K. Tsukiyama-Kohara, A. Katsume, Y. Hirata, S. Sekiguchi, Y. Tobita, Y. Hayashi, T. Hishima, N. Funata, H. Yonekawa, M. Kohara, Pathogenesis of hepatitis C virus infection in *Tupaia belangeri*, J. Virol. 84 (1) (2010) 303–311.
[29] E. Walter, R. Keist, B. Niederöst, I. Pult, H.E. Blum, Hepatitis B virus infection of *tupaia* hepatocytes in vitro and in vivo, Hepatology 24 (1) (1996) 1–5.
[31] L. Li, Z. Li, E. Wang, R. Yang, Y. Xiao, H. Han, F. Lang, X. Li, Y. Xia, F. Gao, Q. Li, N. W. Fraser, J. Zhou, Herpes simplex virus 1 infection of tree shrews differs from that of mice in the severity of acute infection and viral transcription in the peripheral nervous system, J. Virol. 90 (2) (2016) 790–804.
[32] J.P. Li, Y. Liao, Y. Zhang, J.J. Wang, L.C. Wang, K. Feng, Q.H. Li, L.D. Liu, Experimental infection of tree shrews (*Tupaia belangeri*) with Coxsackie virus A16, Zool. Res. 35 (6) (2014) 485–491.
[33] L. Xu, D.D. Yu, Y.H. Ma, Y.L. Yao, R.H. Luo, X.L. Feng, H.R. Cai, J.B. Han, X. H. Wang, M.H. Li, C.W. Ke, Y.T. Zheng, Y.G. Yao, COVID-19-like symptoms observed in Chinese tree shrews infected with SARS-CoV-2, Zool. Res. 41 (5) (2020) 517–526.
[34] L. Xu, D. Yu, Y. Fan, L. Peng, Y. Wu, Y.G. Yao, Loss of RIG-I leads to a functional replacement with MDA5 in the Chinese tree shrew, Proc. Natl. Acad. Sci. U. S. A. 113 (39) (2016) 10950–10955.
[35] D. Yu, Y. Wu, L. Xu, Y. Fan, L. Peng, M. Xu, Y.G. Yao, Identification and characterization of toll-like receptors (TLRs) in the Chinese tree shrew (*Tupaia belangeri chinensis*), Dev. Comp. Immunol. 60 (2016) 127–138.
[36] L. Xu, D. Yu, L. Peng, Y. Fan, J. Chen, Y.T. Zheng, C. Wang, Y.G. Yao, Characterization of a MAVS ortholog from the Chinese tree shrew (*Tupaia belangeri chinensis*), Dev. Comp. Immunol. 52 (1) (2015) 58–68.
[37] L. Xu, D. Yu, Y.L. Yao, T. Gu, X. Zheng, Y. Wu, R.H. Luo, Y.T. Zheng, J. Zhong, Y. G. Yao, *Tupaia* MAVS is a dual target during hepatitis C virus infection for innate immune evasion and viral replication via NF-κB, J. Immunol. 205 (8) (2020) 2091–2099.
[38] L. Xu, D. Yu, L. Peng, Y. Wu, Y. Fan, T. Gu, Y.L. Yao, J. Zhong, X. Chen, Y.G. Yao, An alternative splicing of *tupaia* STING modulated anti-RNA virus responses by targeting MDA5-LGP2 and IRF3, J. Immunol. 204 (12) (2020) 3191–3204.
[39] Y.L. Yao, D. Yu, L. Xu, Y. Fan, Y. Wu, T. Gu, J. Chen, L.B. Lv, Y.G. Yao, Molecular characterization of the 2',5'-oligoadenylate synthetase family in the Chinese tree shrew (*Tupaia belangeri chinensis*), Cytokine 114 (2019) 106–114.
[40] Y.L. Yao, D. Yu, L. Xu, T. Gu, Y. Li, X. Zheng, R. Bi, Y.G. Yao, *Tupaia* OASL1 promotes cellular antiviral immune responses by recruiting MDA5 to MAVS, J. Immunol. (2020), https://doi.org/10.4049/jimmunol.2000740.
[41] T. Gu, D. Yu, Y. Fan, Y. Wu, Y.L. Yao, L. Xu, Y.G. Yao, Molecular identification and antiviral function of the guanylate-binding protein (GBP) genes in the Chinese tree shrew (*Tupaia belangeri chinesis*), Dev. Comp. Immunol. 96 (2019) 27–36.
[42] D. Yu, L. Xu, X.H. Liu, Y. Fan, L.B. Lu, Y.G. Yao, Diverse interleukin-7 mRNA transcripts in Chinese tree shrew (*Tupaia belangeri chinensis*), PLoS One 9 (6) (2014), e99859.
[43] T. Gu, D. Yu, Y. Li, L. Xu, Y.L. Yao, Y.G. Yao, Establishment and characterization of an immortalized renal cell line of the Chinese tree shrew (*Tupaia belangeri chinesis*), Appl. Microbiol. Biotechnol. 103 (5) (2019) 2171–2180.
[44] J.M. Weidner, D. Jiang, X.B. Pan, J. Chang, T.M. Block, J.T. Guo, Interferon-induced cell membrane proteins, IFITM3 and tetherin, inhibit vesicular stomatitis virus infection via distinct mechanisms, J. Virol. 84 (24) (2010) 12646–12657.
[45] J.D. MacMicking, IFN-inducible GTPases and immunity to intracellular pathogens, Trends Immunol. 25 (11) (2004) 601–609.
[46] Y. Hu, J. Wang, B. Yang, N. Zheng, M. Qin, Y. Ji, G. Lin, L. Tian, X. Wu, L. Wu, B. Sun, Guanylate binding protein 4 negatively regulates virus-induced type I IFN and antiviral response by targeting IFN regulatory factor 7, J. Immunol. 187 (12) (2011) 6456–6462.
[47] M.A. Al-Zeer, H.M. Al-Younes, D. Lauster, M. Abu Lubad, T.F. Meyer, Autophagy restricts *Chlamydia trachomatis* growth in human macrophages via IFNG-inducible guanylate binding proteins, Autophagy 9 (1) (2013) 50–62.
[48] D.J. Klionsky, K. Abdelmohsen, A. Abe, et al., Guidelines for the use and interpretation of assays for monitoring autophagy, Autophagy 12 (1) (2016) 1–222.

[49] E.C. Borden, G.C. Sen, G. Uze, R.H. Silverman, R.M. Ransohoff, G.R. Foster, G. R. Stark, Interferons at age 50: past, current and future impact on biomedicine, Nat. Rev. Drug Discov. 6 (12) (2007) 975–990.
[50] G. Wong, X.G. Qiu, Type I interferon receptor knockout mice as models for infection of highly pathogenic viruses with outbreak potential, Zool. Res. 39 (1) (2018) 3–14.
[51] S.P.J. Whelan, J.N. Barr, G.W. Wertz, Transcription and replication of nonsegmented negative-strand RNA viruses, in: Y. Kawaoka (Ed.), Biology of Negative Strand RNA Viruses: The Power of Reverse Genetics, Springer, Berlin Heidelberg, Berlin, Heidelberg, 2004, pp. 61–119.
[52] B.S. Heinrich, Z. Maliga, D.A. Stein, A.A. Hyman, S.P.J. Whelan, Phase transitions drive the formation of vesicular stomatitis virus replication compartments, mBio 9 (5) (2018) e02290–e2317.
[53] T. Kueck, L.M. Bloyet, E. Cassella, T. Zang, F. Schmidt, V. Brusic, G. Tekes, O. Pornillos, S.P.J. Whelan, P.D. Bieniasz, Vesicular stomatitis virus transcription is inhibited by TRIM69 in the interferon-induced antiviral state, J. Virol. 93 (24) (2019).
[54] J. Zhang, R.C. Luo, X.Y. Man, L.B. Lv, Y.G. Yao, M. Zheng, The anatomy of the skin of the Chinese tree shrew is very similar to that of human skin, Zool. Res. 41 (2) (2020) 208–212.
[55] R.J. Ni, Y. Tian, X.Y. Dai, L.S. Zhao, J.X. Wei, J.N. Zhou, X.H. Ma, T. Li, Social avoidance behavior in male tree shrews and prosocial behavior in male mice toward unfamiliar conspecifics in the laboratory, Zool. Res. 41 (3) (2020) 258–272.
[56] Y. Choi, J.W. Bowman, J.U. Jung, Autophagy during viral infection - a double-edged sword, Nat. Rev. Microbiol. 16 (6) (2018) 341–354.
[57] V. Deretic, B. Levine, Autophagy balances inflammation in innate immunity, Autophagy 14 (2) (2018) 243–251.
[58] E. Meunier, P. Wallet, R.F. Dreier, S. Costanzo, L. Anton, S. Ruhl, S. Dussurgey, M. S. Dick, A. Kistner, M. Rigard, D. Degrandi, K. Pfeffer, M. Yamamoto, T. Henry, P. Broz, Guanylate-binding proteins promote activation of the AIM2 inflammasome during infection with Francisella novicida, Nat. Immunol. 16 (5) (2015) 476–484.
[59] E. Kravets, D. Degrandi, Q. Ma, T.O. Peulen, V. Klumpers, S. Felekyan, R. Kuhnemuth, S. Weidtkamp-Peters, C.A. Seidel, K. Pfeffer, Guanylate binding proteins directly attack Toxoplasma gondii via supramolecular complexes, eLife 5 (2016).
[60] S. Park, J. Choi, S.B. Biering, E. Dominici, L.E. Williams, S. Hwang, Targeting by AutophaGy proteins (TAG): Targeting of IFNG-inducible GTPases to membranes by the LC3 conjugation system of autophagy, Autophagy 12 (7) (2016) 1153–1167.
[61] S.B. Biering, J. Choi, R.A. Halstrom, H.M. Brown, W.L. Beatty, S. Lee, B.T. McCune, E. Dominici, L.E. Williams, R.C. Orchard, C.B. Wilen, M. Yamamoto, J. Coers, G. A. Taylor, S. Hwang, Viral replication complexes are targeted by LC3-guided interferon-inducible GTPases, Cell Host Microbe 22 (1) (2017) 74–85 e7.
[62] R. Gosert, D. Egger, V. Lohmann, R. Bartenschlager, H.E. Blum, K. Bienz, D. Moradpour, Identification of the hepatitis C virus RNA replication complex in Huh-7 cells harboring subgenomic replicons, J. Virol. 77 (9) (2003) 5487–5492.
[63] D. Moradpour, F. Penin, C.M. Rice, Replication of hepatitis C virus, Nat. Rev. Microbiol. 5 (6) (2007) 453–463.
[64] M. Yamamoto, M. Okuyama, Ji S. Ma, T. Kimura, N. Kamiyama, H. Saiga, J. Ohshima, M. Sasai, H. Kayama, T. Okamoto, David C.S. Huang, D. Soldati-Favre, K. Horie, J. Takeda, K. Takeda, A cluster of interferon-γ-inducible p65 GTPases plays a critical role in host defense against *Toxoplasma gondii*, Immunity 37 (2) (2012) 302–313.
[65] J. Choi, S. Park, S.B. Biering, E. Selleck, C.Y. Liu, X. Zhang, N. Fujita, T. Saitoh, S. Akira, T. Yoshimori, L.D. Sibley, S. Hwang, H.W. Virgin, The parasitophorous vacuole membrane of *Toxoplasma gondii* is targeted for disruption by ubiquitin-like conjugation systems of autophagy, Immunity 40 (6) (2014) 924–935.
[66] N. Modiano, Y.E. Lu, P. Cresswell, Golgi targeting of human guanylate-binding protein-1 requires nucleotide binding, isoprenylation, and an IFN-gamma-inducible cofactor, Proc. Natl. Acad. Sci. USA. 102 (24) (2005) 8680–8685.

Table S1 Primers used in this study

Gene	Name	Primer sequence (5' - 3')	Application
tGBP1	tGBP1-ΔCaaX F	ATGC***GGATCC***ATGGCCTCAGAGAACCACAT	PCR for constructing pCMV-tGBP1-
	tGBP1-ΔCaaX R	ATGC***CTCGAG***TGTCTTCTTTGGCTTGTCC	ΔCaaX-3Tag-8 using pCMV-3Tag-8 vector
	tGBP1-K51A F	TCTACCGCACAGGCGCCTCCTACCTGATGAAC	PCR for constructing pCMV-tGBP1-K51A-
	tGBP1-K51A R	GTTCATCAGGTAGGAGGCGCCTGTGCGGTAGA	3Tag-8 using pCMV-3Tag-8 vector
VSV-N	VSV-N F	ccggaagatctgagctcgagATGTCTGTTACAGTCAAGAGAA	PCR for constructing pCS2-N-Myc-VSV-N
	VSV-N R	tatagttctagaggctcgagTCATTTGTCAAATTCTGACTTA	using pCS-myc-N vector
	VSV-N F1	gggctgcaggaattcgatatcATGTCTGTTACAGTCAAGAGAATCATTG	PCR for constructing pCMV-VSV-N-3Tag-8
	VSV-N R1	ggtatcgataagcttgatatcTTTGTCAAATTCTGACTTAGCATACTTG	using pCMV-3Tag-8 vector
VSV-P	VSV-P F	tccggaagatctgagctcgagATGGATAATCTCACAAAAGTTCGTGA	PCR for constructing pCS2-N-Myc-VSV-P
	VSV-P R	ctatagttctagaggctcgagCTACCGTAAGGTCTTTCCATGCTC	using pCS-myc-N vector
tIFNB1	tIFNB1 F	ACCACTTGGAAACCATGC	Analytical RT-qPCR for *tIFNB1*
	tIFNB1 R	TTTCCACTCGGACTATCG	Analytical RT-qPCR for *tIFNB1*
β-actin	tβ-actin F	ATTTTGAATGATCAGCCACC	Analytical RT-qPCR for *tβ-actin*
	tβ-actin R	AGGTAAGCCCTGGCTGCCTC	Analytical RT-qPCR for *tβ-actin*
GFP	GFP Rev F	CCAGCAGGACCATGTGAT	Reverse transcription
	GFP F	TACAACTACAACAGCCACAA	Analytical RT-qPCR for *GFP*
	GFP R	CGGATCTTGAAGTTCACCTT	Analytical RT-qPCR for *GFP*
tIFNAR1	tIFNAR1 sgRNA F	CACCGCTCGCCCTCCTATGGGTGA	For constructing CRISPR/Cas9 vector for
	tIFNAR1 sgRNA R	AAACTCACCCATAGGAGGGCGAGC	tIFNAR1 knockout using pX330-T7 vector
	tIFNAR1 Fc	CTCCAGGCATCCCACCAA	PCR for amplifying a region covering
	tIFNAR1 Rc	CACCACCTCCTCCTGTTTGATT	*tIFNAR1* sgRNA targeting

Notes: The nucleotides in italic stand for the site of restriction enzyme, and the nucleotides in the lowercase stand for homologous sequence. The underlined nucleotides were responsible for introducing point mutation. RT-qPCR, quantitative real-time PCR.

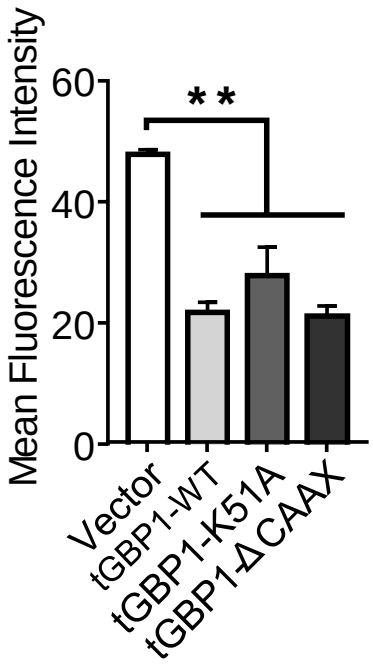

Supplementary Figure 1. Mean fluorescence intensity of GFP in TSPRCs overexpressing wild-type tGBP1 and its mutants. Cells (1×10^5) were transiently transfected with empty vector (Vector), tGBP1-WT (tGBP1), tGBP1-K51A, and tGBP1-ΔCaaX for 12 h, then infected by VSV-GFP (0.01 MOI) for 12 h. Mean fluorescence intensity (MFI) of GFP was analyzed by cytometry. Values are means ±SD (n=2 biological repeats). **, $P< 0.01$, two-tailed Student's *t*-test.

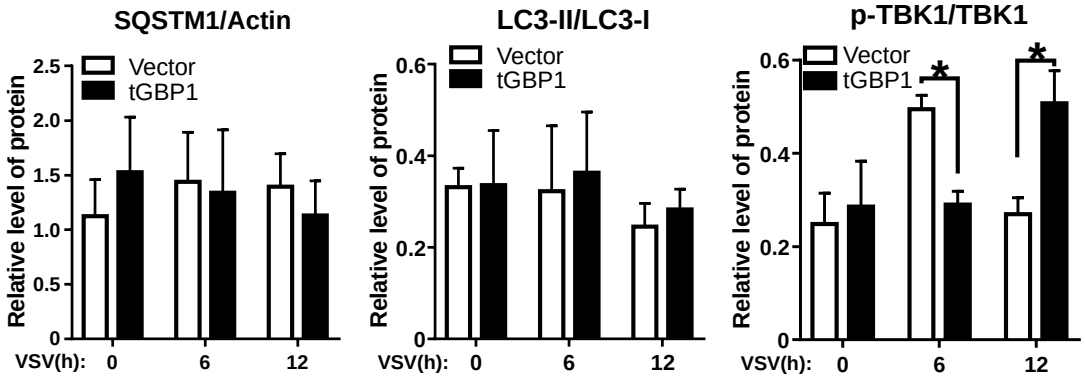

Supplementary Figure 2. Quantification of autophagy-related, p-TBK1, and TBK1 protein levels in TSPRCs based on three independent experiments with similar results. Representative western blotting results are shown in Figure 2B. Values are means ±SD (n=3 independent experiments). *, $P<0.05$, two-tailed Student's *t*-test.

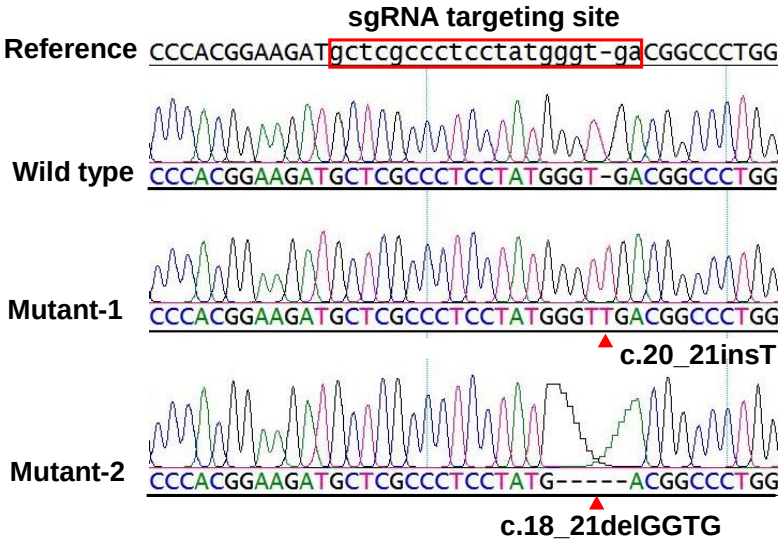

Supplementary Figure 3. Sequencing electropherogram showing CRISPR/Cas9-mediated knockout of tree shrew *IFNAR1* gene in TSR6 cells. sgRNA targeting site is marked by a red box. This cell line harbors two mutations: mutant-1 has an insertion of "T" at target site, and mutant-2 contains a 4 bp deletion at target site. Wild-type cell has a sequence identical to *IFNAR1* gene in reference genome sequence of Chinese tree shrew (www.treeshrewdb.org).

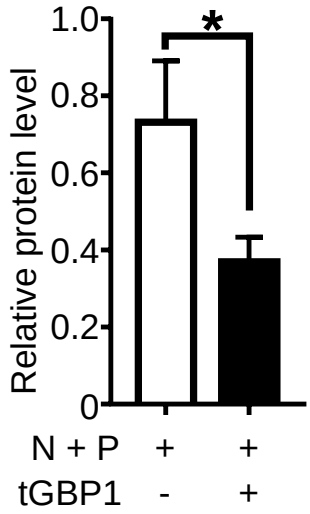

Supplementary Figure 4. Quantification of immunoprecipitated VSV-N protein levels based on two independent experiments with similar results. Protein level of immunoprecipitated VSV-N was quantified and normalized to immunoprecipitated VSV-P. Representative western blotting is shown in Figure 5B. P-pCS2-N-Myc-VSV-P (Myc-VSV-P), N-pCMV-VSV-N-3Tag-8 (Flag-VSV-N), and tGBP1-pCMV-tGBP1-3Tag-8 (tGBP1-WT). Values are means ±SD (n=2 independent experiments). *, $P<0.05$, two-tailed Student's *t*-test.